UNEXPECTED WRINKLING MECHANISM IN THIN WEBS

By

Dilwyn P. Jones
Emral Ltd.
UNITED KINGDOM

ABSTRACT

Wrinkles and creases are a particular problem in thin web materials, leading to functional and visual defects. Their precursor is the wavy pattern in spans between rollers. Troughs running along or close to the machine direction (MD) are always attributed to elastic buckling from compression in the cross direction (CD). In turn, this is caused by width expansion or steering of the web edges inwards. However, the wavy pattern is also seen in sheet specimens under tension, where width contraction is expected from Poisson's ratio. This buckling under applied tension is surprising: it was demonstrated by Friedl et al [1] that CD compressive stress can be generated in the tensile specimens with clamped ends.

This paper uses a linear elastic model for a web span with appropriate web-roller boundary conditions to demonstrate that CD compressive stresses develop if the span length is greater than 0.8 times the width, and the web enters with a CD tension. This may arise from an MD tension rise or spreading on the entry roller. If the compressive stress (assuming the web remains flat) exceeds the critical buckling stress, then troughs are expected to form. The variation of compressive stress with Poisson's ratio, span length and width is explored using the model. Inward microslip near the web edges on the entry roller partly reduces the compression. If the span is too short to develop compression, a reduced effect may be seen in the following span if it is long enough.

An estimate shows that troughs are likely for web thickness of a few 10's of microns and thinner, under MD strain changes of order 0.1%. Post-buckling analysis is not possible with the linear model: however, a beam analogy suggests that the web width may reduce by up to 5 times the linear calculation, and the effect propagates onto the downstream roller. This may allow some troughs to propagate as wrinkles on the roller. This mechanism should be added to the long list of possible causes of wrinkles in thin webs.

NOMENCLATURE

CD	Cross Direction, i.e. along direction of travel
MD	Machine Direction, i.e. along direction of travel
C_1, C_2, C_3, C_4	Fitting coefficients in equation {6}
e	The base of natural logarithms, 2.718
E	Young's Modulus
F	Tension applied to beam
I	Second moment of area of beam
k	Stiffness of beam foundation
L	Span length
L_1, L_2	Lengths of first and second spans
R	Roller radius
t	Web thickness
T	Tension (force per unit width)
u, v	x- and y- components of displacement
W	Web width
x, y	Coordinates in MD and CD
z	Beam displacement
z_b	Beam displacement where foundation buckling occurs
γ	Shear strain
$\Delta\varepsilon_x$	Increase in MD strain
ΔT	Tension increase
ε	Strain
ε_x, ε_y	x- and y- components of strain
ν	Poisson's ratio
σ	Stress
σ_{crit}	Critical CD compressive stress for buckling
σ_x, σ_y	x- and y- components of stress
τ_{xy}	Shear stress

INTRODUCTION

Most webs exhibit some form of wrinkling when transported over rollers on a web line. This is particularly noticeable in webs below 50 μm in thickness, for which the wavy pattern between rollers increases in amplitude and decreases in wavelength. One or more of these "troughs" may form a narrow wrinkle or crease passing around a roller. The sharpness of the crease may be sufficient to yield the material, in which case a visible mark from the crease persists into subsequent spans and the final product. If the crease enters a nip or the wound roll, the pressure may also yield the material, creating a permanent defect. Brittle materials may break, initiated by a crack at the crease. Troughs are normally temporary and non-damaging, but may cause difficulties in thickness measurement, edge sensing and liquid coating. They can be set-in if the web is viscoelastic and it is cooled when they are present. In this paper, the terms "troughs" and "wrinkles" are used interchangeably.

Many web manufacturers, converters and printers use terms like "tension lines" and "draw lines" to describe the trough pattern. By implication, it is attributed to simply applying tension to the web, and guidelines for an upper limit on tension have been presented [2]. At a previous conference in this series, Bosse demonstrated the appearance

of wrinkles when a thin sheet, clamped at both ends, is stretched [3]. This has been erroneously explained by simple Poisson contraction [4,5,6]. These authors stated that cross-direction (CD) compressive stresses accompany the contraction in the width direction. Yet, a rectangular coupon under machine direction (MD) tension and unrestrained in the CD (even at the ends) develops the full width contraction characterized by Poisson's Ratio (see equation {8} below). If there is some restraint from end clamps, or from friction with rollers in a web line, the contraction will be less and so CD *tensile stress* will develop. Compressive stress requires a width reduction larger than the value predicted from Poisson's ratio.

The understanding of wrinkling mechanisms in the web handling community has developed significantly over the past few decades [7]. Wrinkles at an angle to the MD develop as a response to shear when the web is steered [8]. Wrinkles aligned close to the MD develop when the web attempts to expand, or when the edges are steered inwards [7]. One cause of web expansion is the reduction in Poisson contraction accompanying a step *decrease* in tension over a roller. Shelton [9] proposed a wrinkling mechanism whereby a tension *increase* over a roller with poor traction produces wrinkling in the incoming span.

A solution to the problem of wrinkling under tension alone came from a linear stress analysis and finite element modelling of a stretched sheet by Friedl et al [1]. This showed that one or two regions of CD compressive stress could develop, in addition to the strong CD tension near the clamps. There is an "overshoot" of the CD contraction from Poisson's ratio. Cerda et al [10] showed a photo of wrinkles in a stretched polyethylene sheet, and in a later paper [11] linked it to the analysis of [1]. Since then, there have been many publications on theory and experiment in stretched rectangular coupons. However, there has been little more than a hint (see [12]) that this phenomenon would apply to the transport of thin materials.

MODEL FOR A WEB SPAN BETWEEN ROLLERS

This paper extends the previous work to a web travelling between rollers. A linear elastic model has been developed and solved numerically for appropriate boundary conditions. A non-linear model, such as [13], could have been used instead. Finite Element packages are also available, but need to be run forward in time to establish steady state.

The behavior of a rectangular coupon when tension is changed is shown schematically in Figure 1. From its initial state (1) it extends in the machine direction (MD) and contracts in thickness and the cross direction (CD) when tension is applied (2), provided that all the long edges have no forces acting and the short edges are free to contract in the CD. The ratio of CD contraction to MD extension is given by *Poisson's Ratio*. If the tension is partially *reduced* (3), MD extension and CD contraction are both reduced. If the long edges remain free but the left end is clamped after step (2), a zone of CD compressive stress is expected near that end. If the coupon is thin enough, it will not be able to sustain the predicted compression and will buckle instead, forming troughs all the way back to the clamped left end. The edges do not move apart as before: instead the excess width appears in the sinusoidal shape of the troughs.

If instead, the tension is further *increased* (4), without clamping, the MD extension and CD contraction will both increase. Clamping the left end will produce a CD tension in its vicinity, as the width narrows down towards the full contraction. The unexpected behavior is the formation of a region of *CD compressive stress*, approximately one coupon width away from the end. Again, troughs may form in thin coupons, but they do

not extend into the zone of CD tension near the clamp. The edges may again move closer together because of the trough shape.

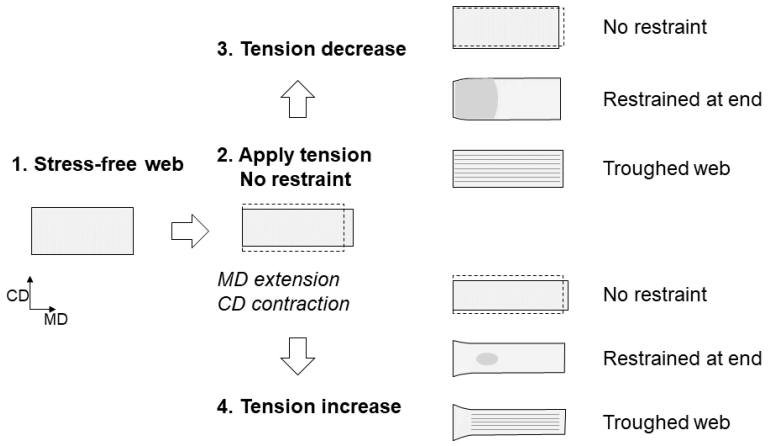

Figure 1 – Applying tension decrease and increase, without and with restraint. End restraint results in compression (shaded) or troughs.

When applied to a web span instead of a coupon, the role of the clamp is performed by friction forces between the web and the entry roller surface. The right end passes onto the exit roller, with boundary conditions discussed below. The edges remain free. Figure 1 therefore represents a tensioned web span. It could also show the left half of a coupon clamped at both ends, with the central line of symmetry at the right end.

Here, we are concerned with solving the "restrained at end" case for a tension increase. With a linear model, solutions can be superposed, so the problem is treated as a superposition of the "no restraint" case, and returning the left end to its starting width. The "no restraint" case has uniform MD extension and stress, uniform CD contraction, and zero CD and shear stresses throughout. It also satisfies the boundary conditions. This leaves the case of uniform CD strain applied to the left end to be solved. This is the same procedure used in the linear model of [1].

Equations

The model starts with basic assumptions commonly used in web handling:

1. The web remains flat, i.e. with no troughs.
2. The web is uniform, with no bagginess.
3. Steady conditions.
4. Inertial effects are negligibly small, which is true for nearly all web lines.
5. The span is therefore in a momentary state of equilibrium.
6. There is no slip between the web and the downstream roller.
7. The web has uniform MD strain and zero CD and shear stress on the upstream roller up to the line of exit.
8. Microslip occurs in a very short area as the web leaves the upstream roller.

The equations are those of linear 2-dimensional elasticity. Equilibrium of stresses gives:

$$\frac{\partial \sigma_x}{\partial x} + \frac{\partial \tau_{xy}}{\partial y} = 0 \qquad \{1\}$$

$$\frac{\partial \sigma_y}{\partial y} + \frac{\partial \tau_{xy}}{\partial x} = 0 \qquad \{2\}$$

x and y are MD and CD coordinates. σ_x, σ_y and τ_{xy} are MD, CD and shear components of stress. The shear stress can be eliminated to give:

$$\frac{\partial^2 \sigma_x}{\partial x^2} - \frac{\partial^2 \sigma_y}{\partial y^2} = 0 \qquad \{3\}$$

Equations {4} to {6} define the MD, CD and shear components of strain respectively, in terms of displacements u and v parallel to x and y.

$$\varepsilon_x = \frac{\partial u}{\partial x} \qquad \{4\}$$

$$\varepsilon_y = \frac{\partial v}{\partial y} \qquad \{5\}$$

$$\gamma = \frac{\partial u}{\partial y} + \frac{\partial v}{\partial x} \qquad \{6\}$$

The web material is taken to be an isotropic linear elastic solid with Young's modulus E and Poisson's ratio ν, obeying the 2-dimensional form of Hooke's Law:

$$\varepsilon_x = \frac{1}{E}\left(\sigma_x - \nu\sigma_y\right) \qquad \{7\}$$

$$\varepsilon_y = \frac{1}{E}\left(\sigma_y - \nu\sigma_x\right) \qquad \{8\}$$

$$\gamma = \frac{2(1+\nu)}{E}\tau_{xy} \qquad \{9\}$$

Equations {4{ to {9} can be combined to give an equation of strain compatibility:

$$\left(\frac{\partial^2}{\partial x^2} + \frac{\partial^2}{\partial y^2}\right)\left(\sigma_x + \sigma_y\right) = 0 \qquad \{10\}$$

Equations {3} and {10} form the basis of the model, to be discretized and solved numerically.

Boundary Conditions

The strains and displacements of the web at the ends of the span are determined by the motion of the entry and exit roller surfaces. The absence of slip over the greater part of the wrap and steady state imply that the velocities of the web and roller surface are matched in direction and magnitude on each roller.

Upstream. It is assumed that the web on the roller is under a lower MD tension than in the model span, and has fully taken up its Poisson contraction so that the CD and shear stresses are zero. The changes to all stress and strain components occur in a microslip zone just before the exit, with friction forces acting. With a high coefficient of friction, the length of the zone is very short, and the displacement components of the web are small. They become zero in the limit of infinite coefficient of friction. This approximation is commonly used in dynamic simulations of MD tension.

At x=0, MD displacement u is zero. Therefore, its second y-derivative is also zero, leading to:

$$\frac{\partial^2 u(0,y)}{\partial y^2} = -\frac{1}{E}\left[(2+\nu)\frac{\partial \sigma_x(0,y)}{\partial x} + \frac{\partial \sigma_y(0,y)}{\partial x}\right] = 0 \qquad \{11\}$$

The actual web width is unchanged as the tension increases by ΔT from that in the previous span. However, the uniform component of the solution gives a contraction as it leaves the roller. Therefore, a width increase equal to the Poisson contraction must be imposed in this component. This is a uniform strain across the width (dependent on web thickness t), leading to:

$$\varepsilon_y(0,y) = \frac{1}{E}\Big(\sigma_y(0,y) - \nu\sigma_x(0,y)\Big) = \frac{\nu\Delta T}{Et} \qquad \{12\}$$

Downstream. There is no microslip at the entry of the downstream roller. The velocity matching condition imposes constant MD strain across the width. This is generally not equal to the nominal MD strain $\Delta T/Et$. Therefore,

$$\frac{\partial \varepsilon_x(L,y)}{\partial y} = \frac{1}{E}\left(\frac{\partial \sigma_x(L,y)}{\partial y} - \nu\frac{\partial \sigma_y(L,y)}{\partial y}\right) = 0 \qquad \{13\}$$

Imaginary particles on the web approach the roller parallel to the MD. This implies that the x-gradient of y-displacement is zero [**Error! Bookmark not defined.**]. Differentiating with respect to y gives:

$$\frac{\partial \varepsilon_y(L,y)}{\partial x} = \frac{1}{E}\left(\frac{\partial \sigma_y(L,y)}{\partial x} - \nu\frac{\partial \sigma_x(L,y)}{\partial x}\right) = 0 \qquad \{14\}$$

Centre Line. The stresses and strains are symmetrical about an MD line in the web center, taken as y=0. This condition is applied to equations {3} and {9} for points (x,0).

Edge. No forces act directly on the edge, so the CD stress is zero there.

$$\sigma_y(x, W/2) = 0 \qquad \{15\}$$

Zero shear stress is applied by integrating equation {1} with respect to y. The model is solving for the additional stresses from stretching the upstream end, but maintaining zero tension. Tension is the y-integral of MD stress, resulting in equation {16}. The x-derivative of equation {16} is also zero, and therefore meets the shear stress condition.

$$\int_0^{W/2} \sigma_x(x,y)dy = 0 \qquad \{16\}$$

Numerical Solution

Equations {3} and {10} to {16} are made non-dimensional by setting both E and the applied CD strain $\varepsilon_y(0,y)$ equal to 1. Then there are only two adjustable parameters, aspect ratio L/W and Poisson's ratio ν.

The equations are solved on a mesh with equal spacing in x and y, and 20 intervals in y between 0 and $W/2$. All derivatives were expressed as 3-point difference equations. The upstream boundary conditions were applied to both corner points (0,0) and (0, $W/2$), the zero CD and shear stress conditions at the edge to the corner (L, $W/2$), and the downstream conditions to the fourth corner (L,0). The resulting simultaneous equations, with 2 unknowns σ_x and σ_y at each mesh point, were solved using the routine RMatrixSolve from the Alglib library for VBA [14]. The model was implemented in an Excel® worksheet using VBA.

Outputs

In addition to the stresses, the displacements $u(L,y)$ and $v(x,W/2)$ were calculated by integrating equations {7} and {8} using the trapezoidal rule. The second of these was used to calculate the change in width along the span.

Verification

The model was not developed further to improve the accuracy around the stress concentrations at the upstream corner (0, $W/2$). A mesh refinement study showed that results converged smoothly towards values within 2% of those obtained with 20 points in y. Run times were typically a few minutes.

A check using the package FlexPDE [15], kindly run by J L Brown, showed that the linear and non-linear elasticity equations gave very similar results.

The model reported here was also adapted to repeat the linear analysis of a stretched sheet in [1]. This involved replacing the downstream boundary conditions ({13} and {14}) by symmetry modifications to equations {3} and {9}. The region solved was now one quarter of the rectangular coupon. The runs reproduced the contour plots and the variation of peak compressive stresses with L/W reported in [1].

MODEL RESULTS

Figure 2 shows contour plots of CD stress σ_y for model runs with aspect ratio L/W = 0.5, 1 and 1.5 and Poisson's ratio of 0.3. As expected, CD stress is tensile close to the upstream boundaries, with the highest values in the corners. It remains tensile throughout the span for the low aspect ratio, but a region of compressive stress develops for the second two cases. Note that the intervals between contours of compressive stress are 50 times smaller than for tension.

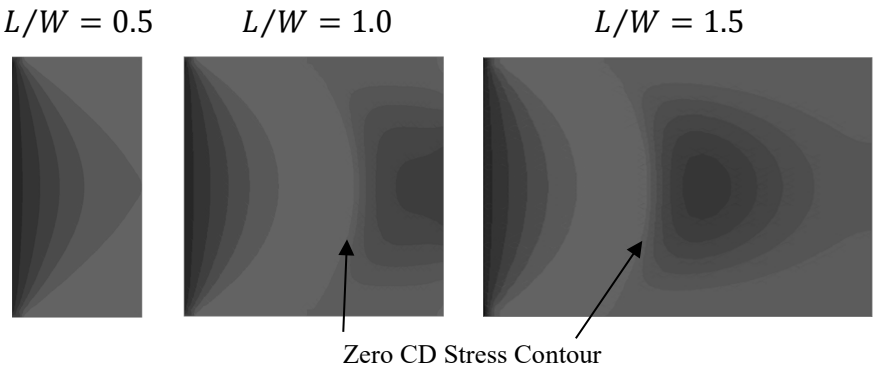

Figure 2 – Model contour plots of CD stress for 3 different aspect ratios. Stress magnitude increases from the lightest shade in steps of 0.05 (tension, left) and 0.001 (compression, left).

The CD stress along the center line is plotted in Figure 3. The expanded view shows it falling below zero for the larger aspect ratios, and displaying a minimum for the largest. The width, calculated from the CD displacement *v*, is plotted in Figure 4 and shows very similar shape curves. Initially, it falls steeply from the imposed CD stretch, and remains higher than the fully Poisson-contracted value for the smallest aspect ratio. However, for the longer spans the width crosses the Poisson-contracted value at around *x/W*=0.6. Beyond that the web is surprisingly narrower, passing through a minimum for the largest aspect ratio.

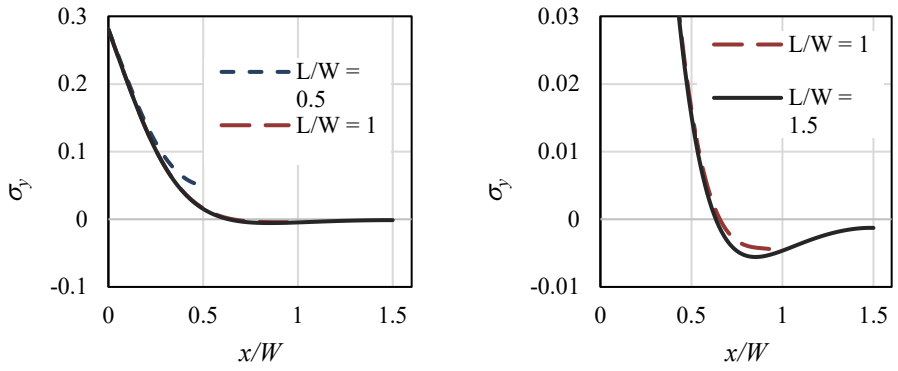

Figure 3 – CD stress along center line for the aspect ratios shown. The right-hand plot is the same but with an expanded y-scale.

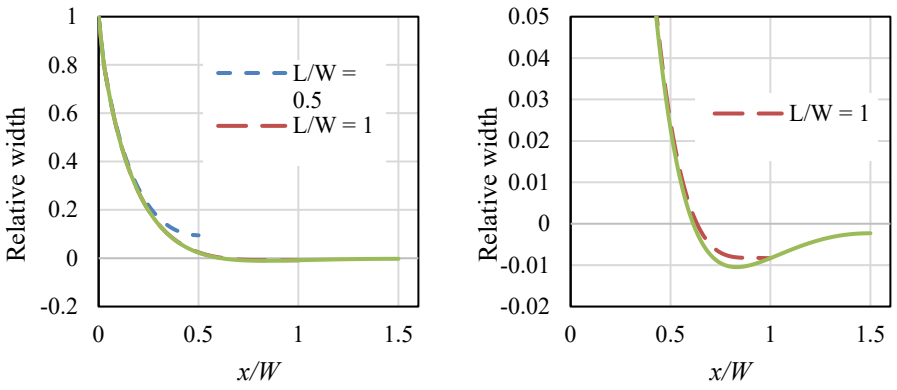

Figure 4 – Width along the span for 3 aspect ratios. The plot on the right is the same but with an expanded y-scale.

Effect of Aspect Ratio

The model was run with several aspect ratios, keeping Poisson's ratio constant at 0.3. Figure 5 shows the lowest value of CD stress (i.e. highest compressive stress) along the center line. A region of compressive stress is present once *L/W* exceeds 0.8, with the largest value at the contact with the downstream roller. At *L/W*=1.05, a minimum appears some distance before the end of the span. As *L/W* increases, that minimum deepens until it reaches a value of -0.056 and a location *x/W* of 0.85 at *L/W*=1.05, then remains at that value as the aspect ratio is increased further. The stress at the end of the span rises, approaching zero by *L/W*=2.

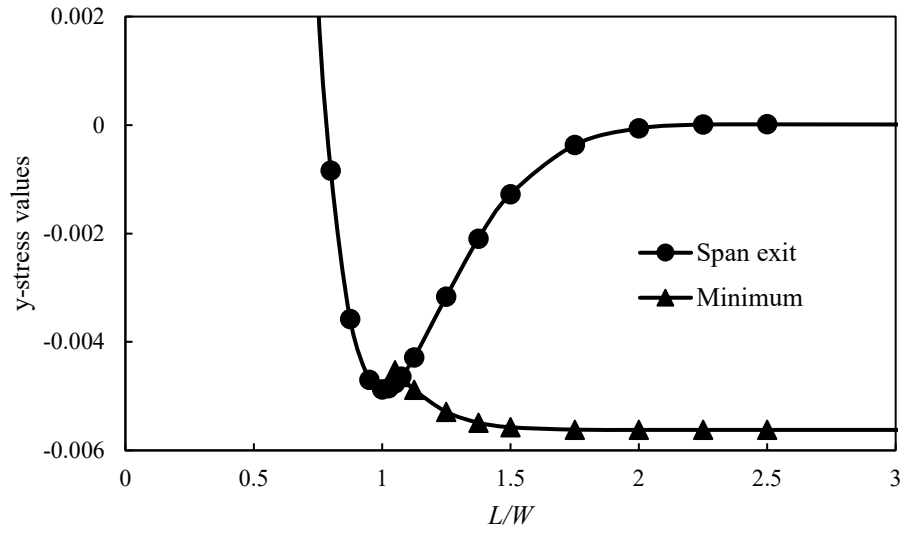

Figure 5 – Minimum stress (highest compressive stress) as a function of aspect ratio, relative to the MD stress change from a tension increase.

Effect of Poisson's Ratio

Figure 6 shows the effect on the minimum stress for an aspect ratio of 1.5 as Poisson's ratio is changed. The magnitude of the stress increases in approximate proportion to Poisson's ratio.

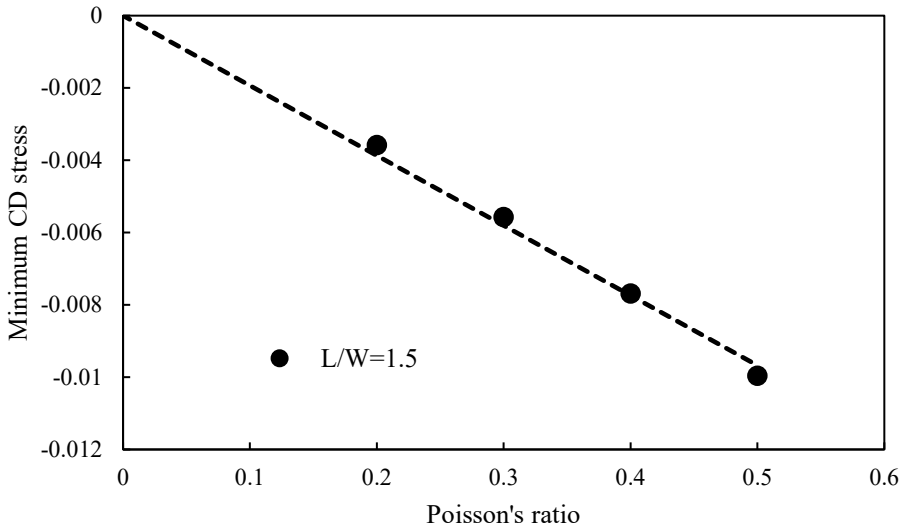

Figure 6 – Minimum CD stress (highest compressive value) plotted versus Poisson's ratio. The line is a linear fit through the origin.

ELASTIC BUCKLING

MD strain from tension is normally under 1% for stiffer webs such as paper, metal foil and polyester, and changes will have similar magnitude. The model results show that CD compressive stress is at most only 0.0056 of MD stress change (for Poisson's ratio of 0.3); i.e. equivalent to a CD strain of order 0.001%. Although this seems dismissively small, it is in fact sufficient to cause a thin web to forms troughs in a span by elastic buckling.

The CD compressive stress from a tension increase is much smaller than that from a decrease of the same magnitude. Then, the CD stress is 0.3 times the MD stress decrease, over 50 times larger.

Threshold

As an example, consider the web in table 1. The MD stress increases from to 5 MPa from 2.5 kPa in the previous span. From the model results, the highest CD compressive stress from this is 14 kPa. By contrast, a tension decrease of 2.5 MPa gives a CD compressive stress of 750 kPa.

Property	Symbol	Value
Young's Modulus	E	5 GPa
Poisson's Ratio	ν	0.3
Thickness	t	20 μm

Span length	L	1 m
Span aspect ratio	L/W	2
Roller radius	R	0.2 m
Tension in span	T	100 N/m
Tension increase from previous span	ΔT	50 N/m

Table 1 – Example parameters for a thin web.

The critical condition for buckling cannot be found easily from this model. Either experiments or a finite element package could be used. However, considering the buckling in the span under uniform MD tension and CD compression [16] has proved useful for analyzing buckling in a web span bending in its own plane, where the actual stresses vary over the area [8]. The analysis can be adapted for many troughs across the width to estimate the critical CD stress as:

$$\sigma_{crit} = \frac{\pi t}{L}\sqrt{\frac{E(T/t)}{3(1-\nu^2)}} \qquad \{17\}$$

For the parameters in Table 1, this is 6 kPa, i.e. well below the predicted CD compressive stress of 14 kPa. Troughs would be expected to form, but at low amplitude. They would only form around the area where compression was predicted, and would be absent from the upstream end of the span where the CD stress is tensile.

The propagation of troughs into narrow wrinkles on rollers has been studied by comparing the CD compressive stress in a web without troughs with a critical buckling stress for a cylindrical shell [16]. Established theory gives that as:

$$\sigma_{crit} = \frac{Et}{R\sqrt{3(1-\nu^2)}} \qquad \{18\}$$

The example in table 1 predicts 320 kPa, well above the expected compressive stress in the span of 14 kPa. Good et al [8,17] found an even larger discrepancy (around 100), which was resolved by using post-buckling analysis.

Post-Buckling Behavior

Stress-strain analysis of sheets containing wrinkles has been carried out in two main ways:

1. Incorporating the out-of-plane displacement and solving the non-linear Kirchhoff-Love plate equations numerically. This requires a very fine grid, with typically 5 or more points in each trough sinewave cycle. Commercial Finite Element packages can be used, as in [1].
2. Using an effective material constitutive relationship, as proposed by Miller and Hedgepeth [18]. Wrinkled regions carry a major principal stress, but the minor component is set to be zero. Taut regions obey the normal constitutive relations, equations {7} to {9}. This was applied to shear wrinkling by Good et al, for misaligned rollers in [8] and tapered rollers in [17]. They carried out a Finite Element analysis of troughing in a span, and showed that the degree of troughing was much greater than the linear analysis predicted. When the web wrapped the next roller without being allowed to buckle, the compressive stress reached the value

predicted by equation {18}. They attributed the occurrence of wrinkles on rollers to this increase in compression post-buckling.

In this paper, an analogy for the web containing MD troughs has been analyzed with similar conclusions. The linear model result for web width at large *L/W* could be fitted very well by a decaying sinusoid with 4 fitting parameters C_1 to C_4 (Figure 7):

$$z = C_4 e^{-C_1 x} \cos(C_2 x + C_3) \qquad \{19\}$$

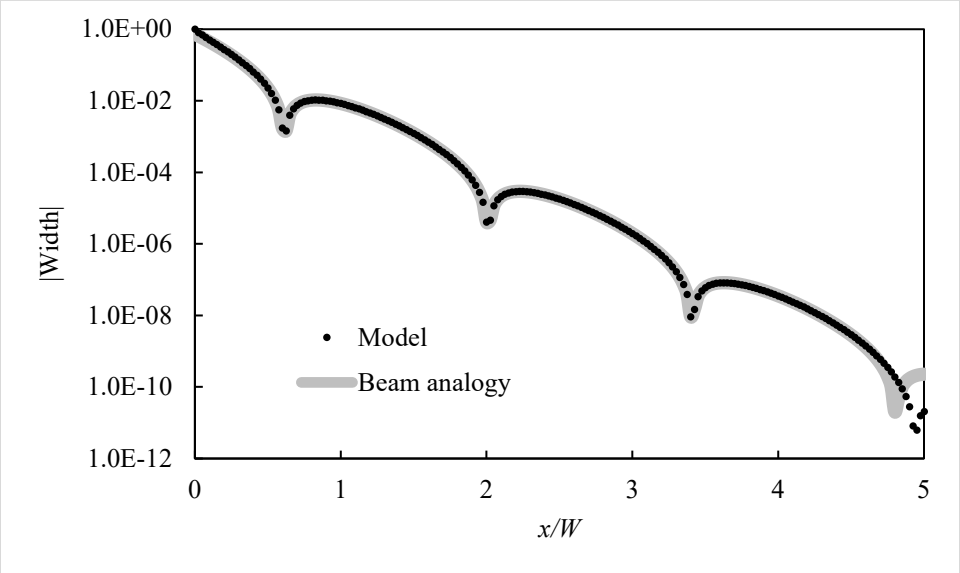

Figure 7 – Model results for width fitted to a decaying sinusoid between *x/W* = 0.6 and 4.5 (avoiding ends).

This is the solution to a fourth-order linear ordinary differential equation. The same equation would be obeyed by a bending beam under axial tensile load *F*, resting on an elastic foundation of stiffness *k*, as shown in Figure 7.

$$EI\frac{dz^4}{d^4x} - F\frac{dz^2}{d^2x} + kz = 0 \qquad \{20\}$$

The ratios of coefficients is determined by C_1 and C_2, whilst C_3 and C_4 give the displacement and slope at x=0.

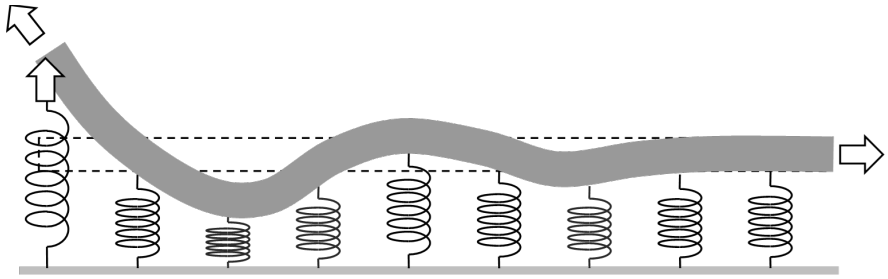

Figure 8 – Analogy for width of troughed web: beam under tension on elastic foundation.

When buckling occurs in part of the span, the CD compressive stress there falls. This can be simulated in the analogy by reducing the restoring force applied by the part of the elastic foundation under compression. The last term in equation {20} is replaced by kz_b, a constant force, in regions where the "buckling threshold" is reached. The case $z_b = 0$ corresponds to the approximation in [18]. A solution is obtained numerically as follows:

1. Set boundary conditions of displacement and slope at x=0 from the L/W = 5 case.
2. Set boundary conditions of zero slope and curvature at x=L
3. Solve equation {17} as written for the beam shape before buckling
4. Replace the last term by kz_b at points where $z < z_b$, and solve again.
5. Repeat step 4 until no points have $z < z_b$.

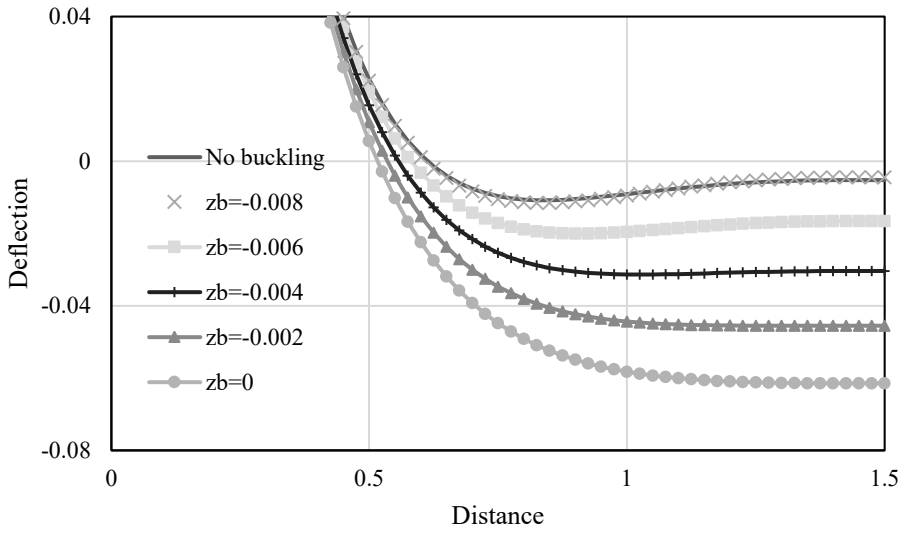

Figure 9 – Deflection versus distance for beam on a buckled elastic foundation as an analogy for the web span.

Figure 9 shows the results of choosing different values of z_b for the case L/W = 1.5. With a buckling threshold just smaller than the minimum deflection, the solution changes little from the unbuckled curve. However, as the threshold is reduced towards zero, the

minimum deflection falls and the length of the foundation which is buckled increases. For zero threshold, the minimum deflection is more than 5 times larger than the non-buckled case.

If these results apply to the web in a span, the extra width reduction would imply a larger amplitude of troughs, and a greater likelihood of wrinkling on a roller, as proposed also by [8].

MODEL REFINEMENTS

Lateral Slip

The compressive stress in the web span model develops because the upstream end is held wider than the Poisson-contracted width by frictional contact with the roller. The uniform CD strain imposed results in finite CD stresses at the web edge on the line of contact. However, this is unrealistic because there is no force acting on the web edge. An approximation by Shelton [19] and developed by the author [20] allows the edges to slide, inwards in this case, to give a linear increase of CD stress until a constant value is reached in the center of the web.

Figure 10 – Trapezoidal variation of CD strain imposed on the upstream end of the span to simulate edge slippage on the roller.

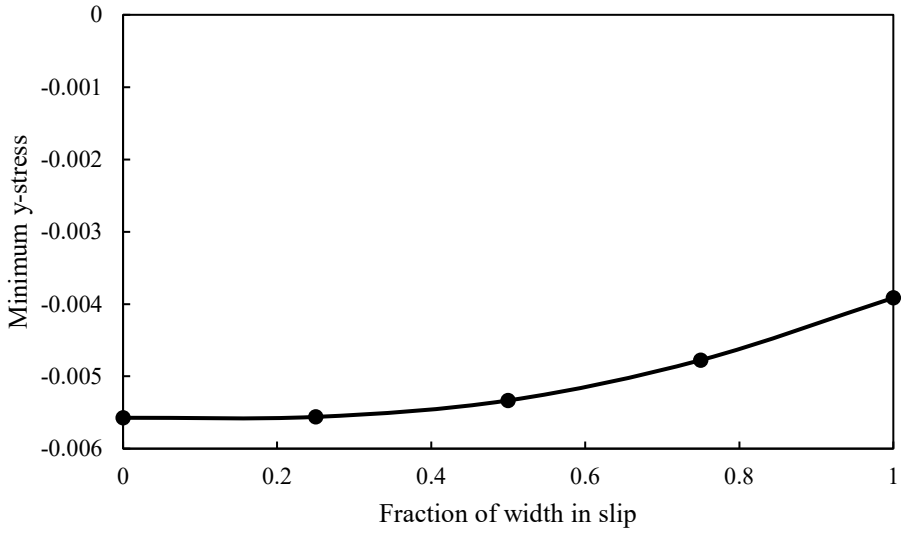

Figure 11 – Effect of edge slippage at the upstream roller on the compressive stress in the span, L/W=0.3, ν=0.3.

This was applied to the web span model by imposing a linear increase in CD strain from the web edge, up to a constant value in the center (Figure 10). The effect on the minimum CD stress is plotted in Figure 11.

The edge slippage has very little effect on the compressive stress until half the width is slipping (i.e. the central half-width is at constant CD strain, roughly as shown in Figure 10). For the last point on Figure 11, the full width is slipping, and the strain distribution is triangular, with a peak value equal to the no-slip strain. This still gives a compressive stress only 30% smaller than for no slip. Further increases in slip keep the triangular strain distribution but reduce the central strain value and the compressive stress in proportion to it.

Consecutive Spans

The compressive stress does not develop in short spans with $L/W < 0.8$. However, the tendency to form the compression is preserved in the variation of CD strain and MD displacement on the downstream roller. Under some conditions, the compressive stress may develop in the next span, even if no further tension change occurs.

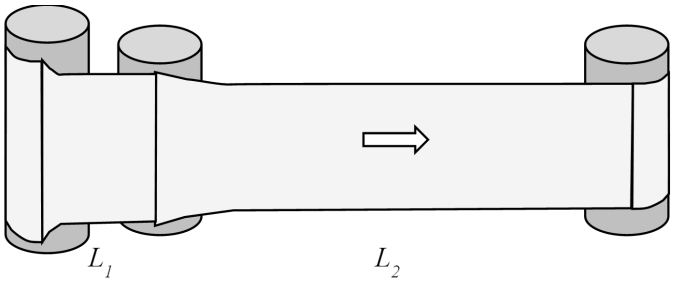

Figure 12 – Model for consecutive spans

This was studied by modelling consecutive spans of length L_1 and L_2. The CD strain and MD displacement as functions of y at the downstream end of the first span were used as the upstream boundary conditions in the second. This shown schematically in Figure 12.

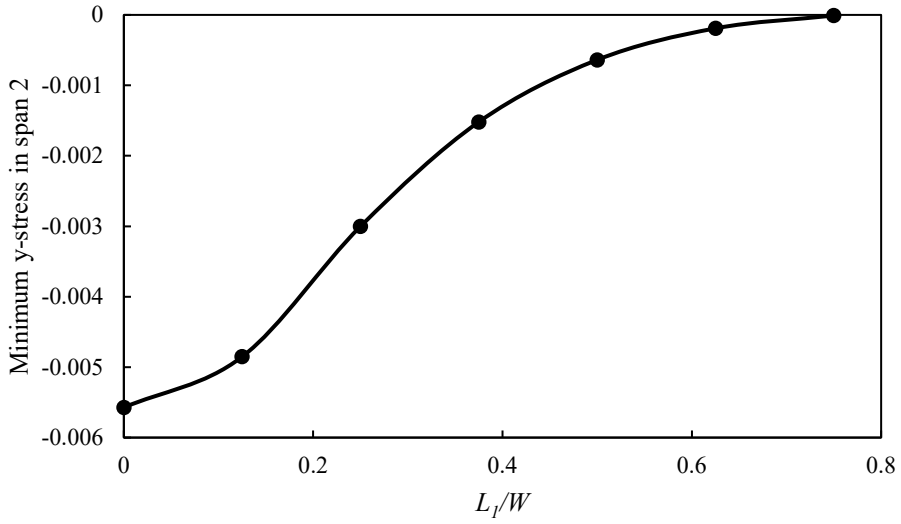

Figure 13 – Variation of maximum compressive stress in second span (L_2/W = 1.5 and ν=0.3) with length of first span.

Figure 13 shows the variation of minimum stress as L_1/W varies, for a fixed value of L_2/W = 1.5. When the first span is short, the compressive stress in the second is only slightly smaller than the single span value. The compressive stress falls as L_1/W increases, and is negligibly small at L_1/W = 0.7. The position of the stress minimum in the second span moves downstream slightly. The consecutive spans do not behave as a single span of length $L_1 + L_2$, but the first one reduces the CD strain at the start of the second.

These runs suggest that spans with aspect ratio around 0.7 are optimal: they do not form troughs themselves, and propagate insufficient CD strain into next span to form troughs there.

FURTHER APPLICATIONS

Spreading Devices

The most obvious alternative application of the model is to a span immediately following a spreading device, even without a tension change. The increase in CD strain relative to that under zero CD stress is equivalent to that caused by the tension increase modelled before. Therefore the conclusion is the same: in spans with $L/W > 0.8$, there will be some CD compressive stress and tendency to form troughs.

The results for short spans show how the effect of spreading falls moving away from the active device. Figure 3 shows that the CD tension is only 20% of its value exiting the spreader for L/W = 0.5, and disappears completely for $L/W > 0.8$.

The model could also be used to model the input span to different types of spreader, as has been carried out by Brown [21]. The model is expected to predict compressive stress a distance $0.85W$ upstream of the spreading device, reproducing his result for a curved axis roller. It may possibly account for observations of folding ahead of a curved axis roller by Shelton [22].

MD Control

Control models for web lines and their implementation in drive controllers [23] normally assume that each span obeys a one-dimensional form of Hooke's Law, relating MD strain and tension:

$$T = Et\varepsilon_x \quad \{21\}$$

Comparison with equation {7} shows that this assumes that the stress in the *y*-direction is zero, in other words, the Poisson contraction is fully achieved through the span. The prediction for the MD strain change for a tension change ΔT is therefore, from equation {21}:

$$\Delta\varepsilon_x = \frac{\Delta T}{Et} \quad \{22\}$$

Yet the actual shape of the web if tension steps up coming into the span from the previous one is shown in Figure 4, and the CD stress in Figure 3 is positive and significant until $x/W = 0.5$. If the tension steps down, the CD stress has the same magnitude but is negative, provided wrinkling does not occur. Many adjacent spans under the same tension will be fully Poisson contracted, but the first span under a higher or lower tension will experience some suppression of the width change expected. This is due to the frictional restraint provided by both upstream and downstream rollers, expressed by the boundary conditions of the model.

If the suppression is complete, the change in CD strain is zero, and equations {7} and {8} can be used to derive the MD strain as:

$$\Delta\varepsilon_x = \frac{\Delta T(1-\nu^2)}{Et} \quad \{23\}$$

For a Poisson's ratio of 0.3, this is 9% smaller than equation {22}. Very short spans cannot develop significant Poisson contraction, so their behaviour is closer to equation {23}.

Control models use equation {21} for the constant MD strain in the span, which is the same as the value contacting the downstream roller. However, the model developed here shows that the MD strain changes rapidly near the upstream roller. For short spans it remains below the value predicted by equation {19} through the whole span length, but reaches it if the L/W is larger than 0.7. Even then, the average MD strain in the span is less than the prediction of equation {22}.

Figure 14 shows the effect of span aspect ratio L/W on the average MD strain in the span, and value in contact with the downstream roller. Both head towards the limit of equation {23} at L/W=0.

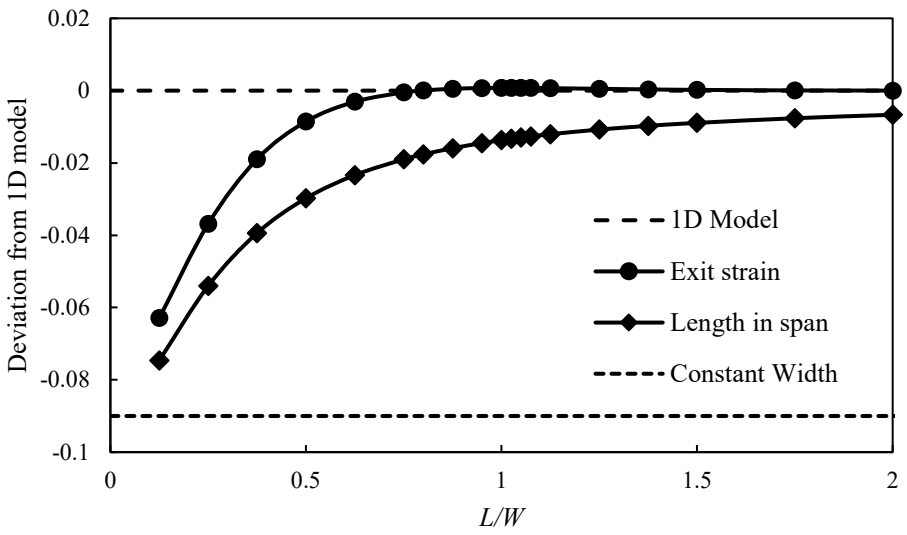

Figure 14 – Deviation from the 1D model for strain change in a span.

For a typical short span with $L/W = 0.25$, the downstream strain is 3.7%, and the average strain 5.4%, below the equation {22} value. These are for a Poisson's ratio of 0.3: the errors will be around 3 times larger as Poisson's ratio approaches 0.5, typical of rubber-like materials.

For both tension increase and decrease, the span appears stiffer than the simple 1D model. Therefore, the relationship between speed, strain and tension normally assumed in drive controls, especially for draw control, will be increasingly in error for spans with low aspect ratio.

CONCLUSIONS

1. There is an unexpected development of compressive stress and tendency to wrinkle in a span after a step up in tension on the upstream roller, or after a spreading device applies a CD tension. The effect is weaker than the well-known effects of web gathering, and expansion after a step down in tension. Nevertheless, the compression can be strong enough to cause troughs in sufficiently thin materials.
2. Troughs are expected to start a distance $W/2$ from the upstream roller, not immediately as in the case of a tension drop.
3. The compressive stress develops in a span with aspect ratio L/W over 0.8, and increases with:
    - Magnitude of tension step
    - Poisson's ratio
    - L/W, up to 1.5, above which it is constant.
4. A low L/W can move the compressive region into the next span at the same tension. The optimum L/W after a tension step up is 0.7, with no compression in that span or the next.
5. Inward web-roller slip at the edges has little effect on the compressive stress.

6. Thick materials will support the compression without forming wrinkles, but when thin webs wrinkle the edges will move further in and increase the wrinkle amplitude.
7. This work reports likely post-buckling behavior with a model analogue of a beam under tension on a variable elastic foundation. More accurate modelling would incorporate the flattening of wrinkles approaching the downstream roller.
8. The 2D web span model provides insight into wrinkling, retention of CD tension after spreading, and the tension-speed behavior of a short web span.

ACKNOWLEDGEMENTS

I would like to thank Jerry Brown for running his model to check the results are similar.

REFERENCES

1. Friedl, N., Rammerstorfer, F. G., & Fischer, F. D., "Buckling of Stretched Strips," Computers and Structures, Vol. 78, 2000, pp. 185-190.
2. E.g. Stewart, J., "Principles of Thin Film Handling," Proceedings of the AIMCAL 1994 Fall Technical Conference on Web Handling and Thin Film Handling, 1994, pp. 1-54.
3. Bosse, R., "Permanent Out-of-Plane Distortions of Paper Printed in Heat-Set Web Offset," Proceedings of the Fifth International Conference on Web Handling, Ed. Good, J. K., Oklahoma State University, 1999, pp. 355-373.
4. Hawkins, W. E., The Plastic Film and Foil Web Handling Guide, CRC PRESS, Boca Raton, USA, 2003.
5. Hashimoto, H., Theory and Application of Web Handling, Converting Technical Institute, Tokyo, Japan, 2015.
6. Martz, Y., and Knittel, D., "Dynamics of an Elastic Web in Roll-to-Roll Systems Using Finite Element Method," Proceedings of the 11th World Congress on Computational Mechanics (WCCM XI), 5th European Conference on Computational Mechanics (ECCM V) and 6th European Conference on Computational Fluid Dynamics (ECFD VI), Ed. E. Oñate, E., Oliver, J. and Huerta A., Barcelona, Spain, 2014.
7. Roisum, D. R., "The Mechanics of Wrinkling," TAPPI Journal, Vol. 79, 1996, pp. 217-226.
8. Good, J. K., Beisel, J. A., and Yurtçu, H. H., "Predicting Web Wrinkles on Rollers", Proceedings of the Tenth International Conference on Web Handling, Ed. Good, J. K., Oklahoma State University, 2009, pp. 495-530.
9. Shelton J. J., "Buckling of Webs from Lateral Compressive Forces", Proceedings of the Second International Conference on Web Handling. Ed. Good, J. K., Oklahoma State University, 1993, pp. 303-321.
10. Cerda, E., Ravi-Chandar, K., and Mahadevan, L., "Wrinkling of an Elastic Sheet under Tension," Nature, Vol. 419, 2002, pp. 579-580.
11. Cerda, E., and Mahadevan, L., "Geometry and Physics of Wrinkling," Physical Review Letters, Vol. 90, No. 7, 2003, p. 074302.
12. Fischer, F. D., Rammerstorfer, F. G., Friedl, N., and Wieser, W., "Buckling Phenomena Related to Rolling and Levelling of Sheet Metal," Int. Journal of Mechanical Sciences, Vol. 42, Issue 10, 2000, pp. 1887-1910.

13. Brown, J. L., “A New Method for Analyzing the Deformation and Lateral Translation of a Moving Web,” Proceedings of the Eighth International Conference on Web Handling, Ed. Good, J. K., Oklahoma State University, 2005, pp. 39-59.
14. ALGLIB (www.alglib.net), Sergey Bochkanov and Vladimir Bystritsky.
15. FlexPDE from PDE Solutions Inc, 9408 E. Holman Rd., Spokane Valley, WA 99206, USA. www.pdesolutions.com.
16. Timoshenko, S. P., and Gere, J. M., Theory of Elastic Stability, McGraw Hill, New York, 1961.
17. Yurtçu, H. H., Beisel, J. A., and Good, J. K., “The Effect of Roller Taper on Webs,” TAPPI Journal, Vol. 11, Issue 11, 2012, pp. 31-38.
18. Miller, R. K., and Hedgepeth, J. M., “An Algorithm for Finite Element Analysis of Partly Wrinkled Membranes,” AIAA J., Vol. 20., Issue 12, 1982, pp. 1761-1763.
19. Shelton J. J., “Buckling of Webs from Lateral Compressive Forces,” Proceedings of the Second International Conference on Web Handling, Ed. Good, J. K., Oklahoma State University, 1993.
20. Jones, D. P., and McCann, M. J., “Wrinkling of Webs on Rollers and Drums,” Proceedings of the Eighth International Conference on Web Handling, Ed. Good, J. K., Oklahoma State University, 2005, pp. 123-140.
21. Brown, J. L., “Effects of Concave Rollers, Curved-Axis Rollers and Web Camber on the Deformation and Lateral Translation of a Moving Web,” Proceedings of the Eighth International Conference on Web Handling, Ed. Good, J. K., Oklahoma State University, 2005, pp. 61-80.
22. Shelton, J. J., “Interaction between Two Web Spans Because of a Misaligned Downstream Roller,” Proceedings of the Eighth International Conference on Web Handling, ed. Good, J. K., 2005, pp. 101-120.
23. E.g. Shin, K-H., Tension Control, TAPPI Press, Atlanta, 2000.